Short and ultrashort laser pulse induced bubbles on transparent and scattering tissue models.

Francisco Pérez-Gutierrez[1], Rodger Evans[2], Santiago Camacho-Lopez[2], Guillermo Aguilar[1].

1. University of California, Riverside
900 University Ave. Riverside, CA, 92521, USA
2. Centro de Investigación Científica y Educación Superior de Ensenada
Km. 107 Carretera Tijuana-Ensenada, Ensenada, B.C., Mexico

ABSTRACT

Bubble formation is a well identified phenomenon within short (ns) and ultrashort (fs) laser pulses-aqueous media interactions. Bubble formation might be produced by three different mechanisms: (1) optical breakdown, (2) rarefraction wave and (3) overheating of the material. Experiments where transparent and scattering tissue models that mimic biological tissue were irradiated with a Q-switched, 532 nm, 5 nanosecond, Nd:YAG and Ti:sapphire femtosecond laser systems. The type of bubble (transient or permanent) and initial bubble diameter were characterized as a function of time as well as the number of pulses and repetition rate at which they were delivered. Threshold fluence for bubble formation in scattering tissue model was also studied. Two types of bubbles were identified depending on the number of pulses and the repetition rate at which they were delivered: transient (type 1) and permanent (type 2) bubbles. There is an insignificant difference in the fluence required to form a bubble in transparent tissue models regardless of the depth at which the beam was focused; in contrast, for scattering tissue models, the fluence required to form a bubble in deep positions is significantly higher than that of more superficial beam focus positions.

1. INTRODUCTION

Since it was invented, almost 50 years ago, the laser has been widely used for many applications in the field of medicine; both continuous wave (CW) and pulsed lasers are suitable for medical applications[1]. The physical mechanisms involved in a laser-matter interaction depend, apart of wavelength, on the pulse intensity, which itself depends on the laser pulse duration; the shorter the pulse the higher the peak intensity. Long laser pulses (ns to ms) couple its energy to the material mainly through the wavelength dependent linear absorption, according to an extinction coefficient (μ_t); most of the energy deposited to the material produces heat and, therefore, the interaction is dominated by heating phenomena. When the laser pulse is very short (below 10ps and down to a few fs), a fast optical and avalanche ionization process dominates the interaction and an expanding plasma is produced with very small amounts of heat transferred to the targeted material[2]. Ultrashort laser-matter interactions are, to a certain degree, wavelength-independent. While for certain transparent materials like glass there exist two distinctive "and definite trends" for the damage threshold fluence of the material for laser pulse durations above and below 10ps [3], the frontier between long and ultrashort pulses is not very well established in the context for all materials, particularly biological ones.

Long laser pulses (ms to μs) at convenient wavelengths have been incorporated (and sometimes combined with other tools) to laser surgeries where the aim is to produce thermal (by laser heating) treatment of specific chromophores and/or tissue ablation[4]. However, there are specific cases where the treatment is not totally successful; as an example, Port Wine Stain (PWS) birthmarks are an abnormal layer of blood vessels 10 to 100μm in diameter localized 100 to 500 μm below the skin surface, that have been treated using long (1 to 2ms) laser pulses in combination with Cryogen Spray Cooling (CSC). The aim of this treatment is to achieve the temperature at which blood in the vessel coagulates at the same time that the other chromophores in the skin remain undamaged; this treatment has proved successful with large blood vessels (100μm) because they have a long thermal relaxation time (5ms) that allows thermal confinement in the blood vessel, hence achieving the coagulation temperature; in contrast, smaller blood vessels (10μm) have shorter

Optical Interactions with Tissue and Cells XVIII, edited by Steven L. Jacques, William P. Roach,
Proc. of SPIE Vol. 6435, 64350V, (2007) · 1605-7422/07/$18 · doi: 10.1117/12.701566

thermal relaxation time (50μs), which does not allow sufficient thermal confinement, hence the laser heat produced during the pulse quickly diffuses away to the surrounding tissue before the coagulation temperature is achieved and the blood vessel remains undamaged. A feasible solution for this problem is the use of shorter (nanoseconds, picoseconds to femtoseconds) laser pulses that deliver its energy faster than the thermal relaxation time of those small vessels. We expect to create the conditions for fast laser heating, but also for additional mechanical phenomena triggered by the laser-tissue interaction such as cavitation and shockwaves, which might contribute to the damage and elimination of the very small blood vessels which are difficult to remove by slow laser heating.

Several authors have observed that when laser pulses of μs and shorter are focused on aqueous media a bubble is formed[5,6,7,8]; its diameter and lifetime strongly depend on the laser parameters and material properties, but the conditions for bubble formation must be determined in each individual case. There are three different possible mechanisms for bubble formation: (1) optical breakdown, (2) rarefraction wave and (3) overheating of the material (Laptko, 2006). The bubble formation contributes to material ablation and has found applications in medical procedures such as laser angioplasty and ophthalmic surgeries.

In the initial stage of our work, experiments focusing a 5 ns, Nd:YAG laser beam on a vascular lesion artificial model were carried out [9]. The threshold fluence for bubble formation was found for different absorption coefficients when the laser beam was focused at a specific depth below the surface; also, the characterization of the bubble diameter as a function of fluence was carried out for several samples with different absorption coefficients, however, only permanent bubbles were studied. In the present work the main objectives are to study the bubble dynamics, i.e., its formation and evolution when a series of pulses at three different repetition frequencies are delivered using a fluence value close to the threshold fluence and, to find the threshold fluence for bubble formation in a scattering tissue model. The last study intends to mimic a highly scattering tissue, like skin. Our experiments were carried out using a 532 nm, Nd:YAG laser, pulse duration of 5 nanoseconds and a 90 femtosecond laser.

2. MATERIALS AND METHODS

2.1 Artificial Tissue Models

Agar is typically a strong gelling polysaccharide derived from red seaweeds. Agar solutions gel due to the presence of the agarose fraction of the crude agar at common concentrations between 0.5 and 2.0%. Agar typically needs to be heated above 90 ºC to liquify (melt) and depending on the seaweed source the setting temperature can be between 30 and 45 ºC. As agar gels are mainly conformed by water, they are an excellent material to make artificial tissue phantoms. They may also be combined with other substances to approximate its optical properties to more realistic tissue. In this work, two types of agar phantoms were used. Figure 1 shows the first model, which is made of a single 500 μm thick layer of transparent agar, it was used for the experiments where the bubble dynamics were studied for different number of pulses and repetition rates. Note that the beam was focused 100μm below the surface. Figure 2 shows the second model, which we used to study the bubble formation in a highly scattering medium. It is composed by two layers. The top 254 μm thick layer, the scattering one, is constituted by a mixture of liquid agar gel and 4.8% intralipid; the scattering layer was stacked on top of another layer made of transparent agar gel. For this case the laser beam was focused at 50, 100 and 200 μm deep in the scattering layer.

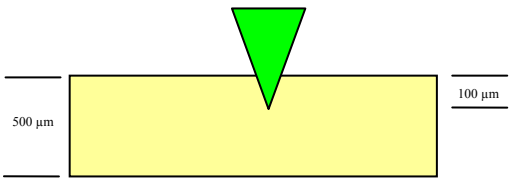

Figure 1. 500 μm thickness transparent agar single layer.

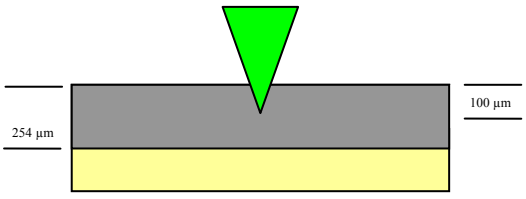

Figure 2. Highly scattering agar layer stacked on top of another layer of transparent agar.

2.2 Experimental setup and bubble detection

The experimental set up is shown in Figure 3. It can be used in a configuration that includes both a 532 nm, Nd:YAG, 5 nanosecond pulses as well as a 810 nm, Ti:Sapphire, femtosecond as excitation beams and a 632.8 nm HeNe continuous wave laser as probe beam, which are focused on the target with a 0.5 NA, 8 mm focal length aspherical lens that we will call the microprocessing lens. The energy per pulse delivered on target is monitored either with a properly calibrated photodiode and an oscilloscope or directly with an energy head detector. A CCD camera is used to capture the image of the focused beam on the target; this is done by using an image relay system constituted by the microprocessing lens and the 500mm lens shown in Fig. 3; the light that reflects backwards from the surface is collected by the two lenses projecting an image of the beam waist on to the CCD. This image relay system provides three very useful features to our set up: (1) it requires normal incidence to work so that the sample surface is always perpendicular to the incident beam, and therefore, in the event of a transversal scan of the sample the beam waist of the focusing light stays always at a constant distance from the surface; (2) it allows fine positioning of the beam waist right on the surface of the sample, and hence at a know depth within the layer, with a resolution of the order of the Rayleigh range of the focusing beam, and; (3) the same image relay system allows to record movies of the bubble formation and evolution inside the agar gel. The bubble formation dynamics is also recorded by use of the HeNe probe beam; the light transmitted through the sample is collected onto a photodiode connected to a data acquisition system. If the bubble is not present, the HeNe light detected by the photodiode produces a constant signal, however, when the bubble forms the initial constant signal drops to a minimum (when the bubbles reaches its maximum diameter) and it recovers back up as the bubble collapses.

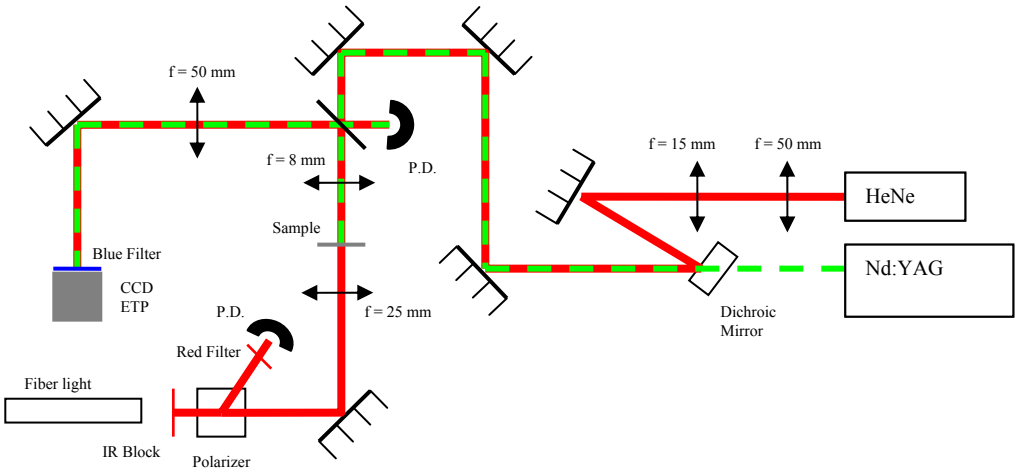

Figure 3. Experimental Setup

2.3 Image processing

Movies of the laser-induced bubbles were taken at 10 frames per second and split into several pictures. The diameter of the bubble was measured for a selected number of pictures using a standard image processing software (ImageJ). Figure 4 shows a typical sequence of photos of the bubble image obtained on the CCD camera.

3 RESULTS AND DISCUSSION

3.1 Bubble dynamics

Figures 5 to 9 contain experimental results of laser irradiation of agar gel models with laser pulses of 5ns duration, at a wavelength of 532 nm, on a 500 µm thick transparent layer. The beam was focused 100µm deep in the agar gel layer. The data point plotted at t=0 represents the diameter of the bubble right after the last pulse. All these experiments were

carried out with fluence slightly smaller than that for the bubble formation threshold (240 J/cm^2) for permanent bubbles (220.6 ± 9.6 J/cm^2) such that we could generate the transient bubbles we are interested in; the fluence values shown in figures 5 to 9 correspond to the average fluence value of the total number of pulses applied.

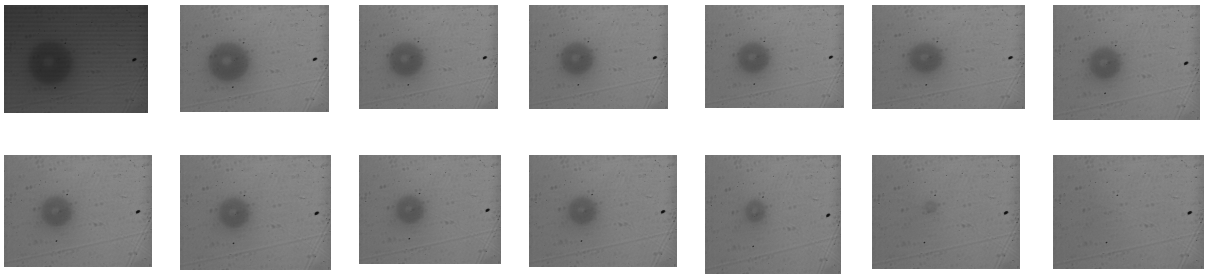

Figure 4. Typical sequence of photos that describe how the bubble diameter changes with time. The bubble was obtained by using a single 5 ns (532nm) Nd:YAG laser pulse with fluence of 204.65 J/cm^2. Upper row (left to right): 0 s, 0.4 s, 1.06 s, 1.73 s, 2.4 s 3.06 s, 3.77 s. Lower row (left to right): 4.4 s, 5.06 s, 5.73 s, 6.4 s, 9.7 s, 13.06 s, 15.5 s.

Figure 5 shows the time evolution from maximum bubble diameter when a single laser pulse is applied, each curve corresponds to different applied fluences, which are in fact obtained from the inherent fluctuation of the laser system. Except for one case (199.16 J/cm^2), it was found that the higher the fluence, the bigger the bubble size and that the bigger the bubble, the longer the life-time of the bubble. The case that falls off the typical trend seen for the other cases might be explained by an inhomogeneous agar gel sample. This is also suggested by the fact that for some experiments the bubble was not formed. Figure 5 just shows those cases where the bubble was formed

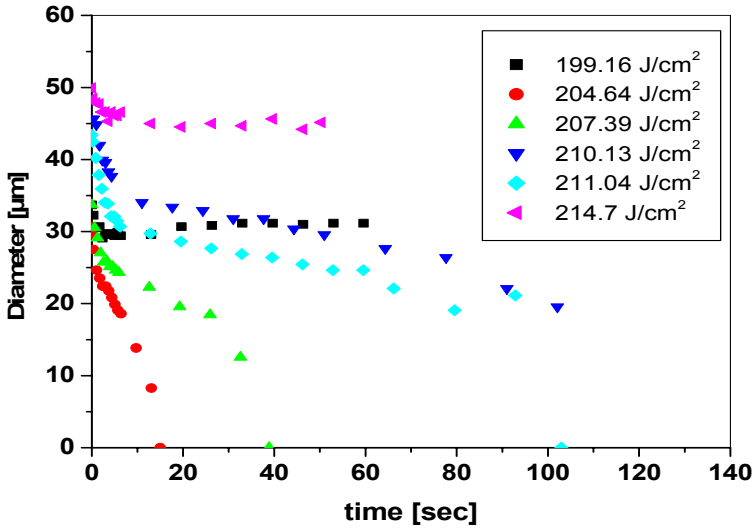

Figure 5. Bubble diameter evolution when the bubbles are created by a single 5 ns Nd:YAG laser pulse at 532nm.

Figures 6 to 9 contain the evolution of the bubble diameter for bubbles formed by a different number of pulses (1 to 10) at three different repetition rates (1, 2 and 3 Hz). Two types of distinctive bubbles were obtained: Figures 6 and 8 show the typical trend for the **type 1** bubbles which are transient and, therefore, they shrink until they fully disappear. The data point with diameter equal to zero is missing in the plot, this is due to the lack of screen resolution to measure the bubble at the exact instant when the bubble collapses completely. Figures 7 and 9 show the **type 2** bubbles, which experience some shrinkage at the beginning, but they manage to remain at constant diameter in the agar gel for long periods of time. For the evolution of the **type 1** bubbles, it is possible to distinguish three different slopes that indicate

the rate at which the bubble diameter collapses at different times, while in the case of the **type 2** bubbles only two slopes are distinguished after the bubbles have formed. We must point out that in many cases, where several pulses were delivered, the average fluence value is not directly proportional to the initial bubble diameter as it is the case when a single pulse was delivered to the target (Fig. 5), this may be due to the fact that the shown value is the *average* fluence taken from all the applied pulses, but it is the pulses with higher fluence the ones that dominate the final size of the bubbles. We have cases where the delivery of 10 pulses at 2 and 3 Hz repetition rate resulted in rather too large bubbles, which could not be measured with the current experimental setup. Table 1 summarizes the type of bubble formed in all the experiments according to the number of pulses and the repetition rate and fluence used. It can be clearly seen from table 1 that when the pulses are delivered at 1Hz it takes 10 consecutive pulses for the bubble to start to behave as a type 2 bubble, otherwise, the bubbles behave always type 1 bubbles; while in the case when pulses are delivered at 3 Hz all the bubbles, even those formed with just a couple of pulses, are permanent (type 2).

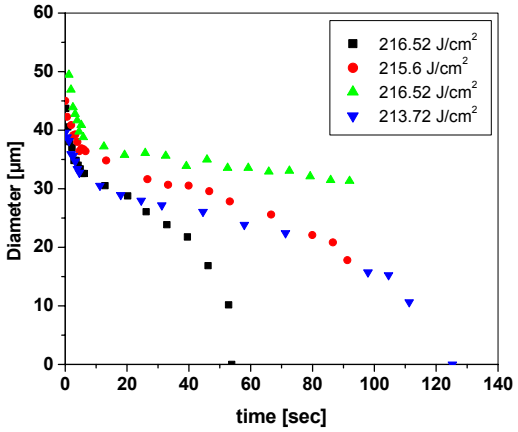

Figure 6. Bubble dynamics when 6 pulses at 1 Hz are applied.

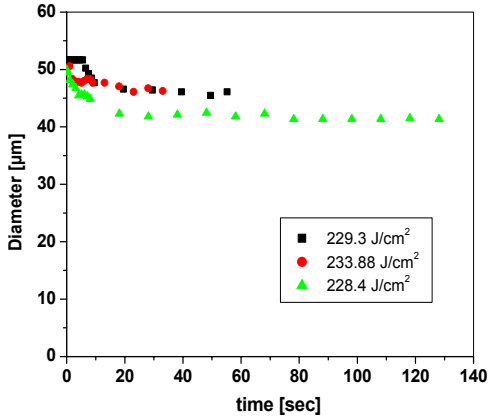

Figure 7. Bubble dynamics when 10 pulses at 1 Hz are applied.

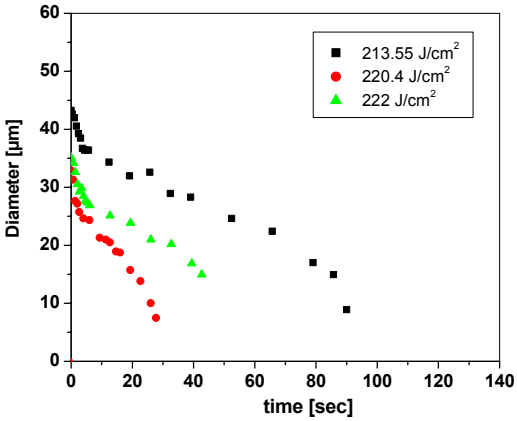

Figure 8. Bubble dynamics when 2 pulses at 1 Hz are applied

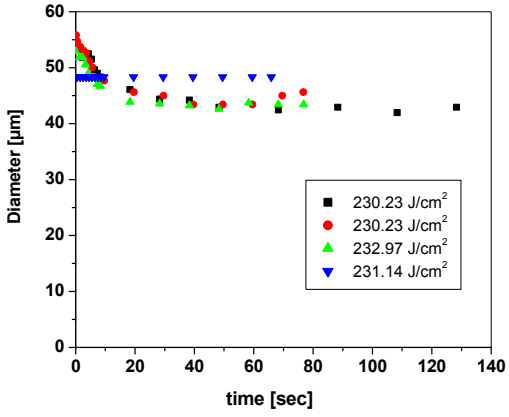

Figure 9. Bubble dynamics when 2 pulses at 3 Hz are applied

Figures 10 and 11 describe the initial bubble diameter as a function of the number of pulses and the repetition rate at which the pulses were delivered on the target, respectively; error bars were added when calculation of standard deviation was possible from the experimentally acquired data. It can be seen from the plots and the experimental observation (Table 1) that there is a slight tendency of the bubble diameter to increase with the number of pulses at 1Hz

and with repetition rate. This variation is more significant when 10 pulses are applied; unfortunately, this cannot be plotted in figures 10 and 11 because we were unable to measure those large bubbles, as mentioned above.

	Frequency		
Number of pulses	**1 Hz**	**2 Hz**	**3 Hz**
1	1	-	-
2	1	1	2
3	1	1	2
6	1	2	2
10	2	NM	NM

Table 1. Summary of bubble type obtained when different number of pulses at three different repetition rates. The type 1 bubble completely collapses with time; the type 2 bubble remains at a constant diameter in the agar gel. NM: means the bubble was too large to be measured with our current set up.

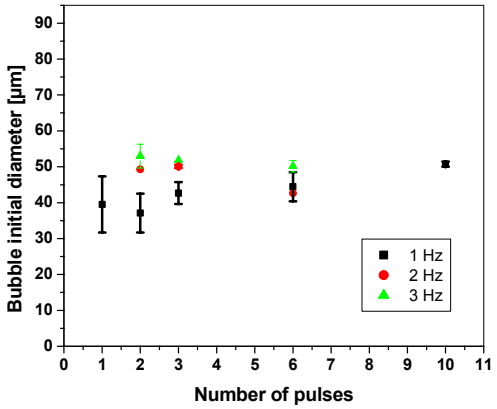

Figure 10. Initial bubble diameter as a function of number of pulses

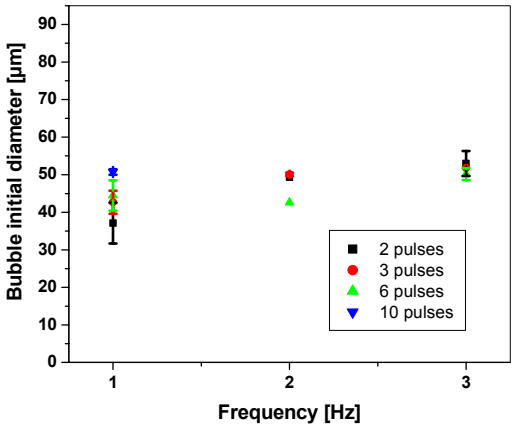

Figure 11. Initial number of pulses as a function of repetition rate.

3.2 Effect of Scattering.

Figures 12 and 13 show plots that compare the laser fluence required to form a bubble with a 5 ns laser pulse at three different depths in transparent and highly scattering agar gel, respectively. From Figure 12, it can be seen that there is insignificant difference in the fluence required to produce the bubble in transparent agar, regardless of the depth at which the beam is being focused; notice also that there is no a defined value for bubble formation threshold fluence, which is indicated by the overlapping of the fluence error bars for the bubble and no-bubble formation events. Figure 13 shows the data for bubble formation in highly scattering agar. It can be seen that in this case too, the laser fluence difference for the bubble and no-bubble formation is very small, although only for the cases where the laser beam is focused at depths of 50 and 100 µm. However, this laser fluence difference becomes larger if the laser beam is focused 200µm deep.. It is also clear from comparison of Figs. 12 and 13 that the formation of all bubbles in the scattering agar requires larger fluences (on the order of 50% higher fluence) as compared to the formation of bubbles in transparent agar, especially for the 200µm deep case, where up to 3 times higher fluence is required.

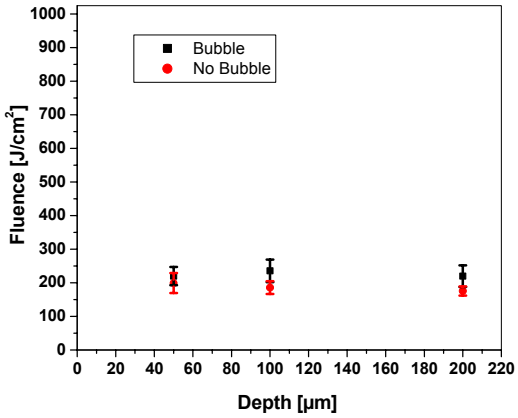

Figure 12. Laser fluence required to form a bubble in transparent agar at different depths.

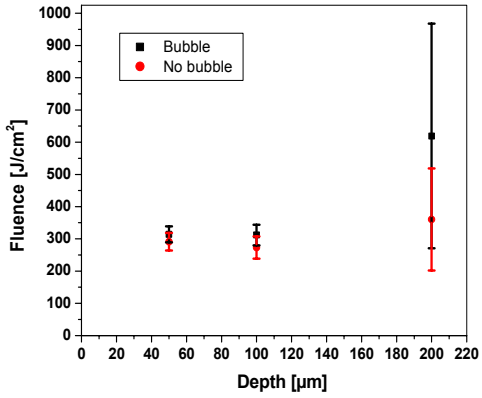

Figure 13. Laser fluence required to form a bubble in scattering agar at different depths.

3.3 Irradiation with femtosecond laser pulses.

Similar experiments were carried out irradiating transparent agar gels with bursts from Ti:Sapphire femtosecond laser pulses positioning the focal point 100µm below the gel surface, the variation of the bubble size with time is shown in Figure 14; the maximum energy used for these experiments was the maximum energy that was available with the laser system at the moment of the experiment. The fluence value shown in Figure 14 for each curve is the average fluence of two burst that produced the bubble. It should be noticed that the initial size of the bubbles is half of the maximum size obtained with nanosecond laser pulses and that all of these bubbles collapse within 20 seconds, in contrast with those produced by nanosecond laser pulses. No permanent bubbles were observed.

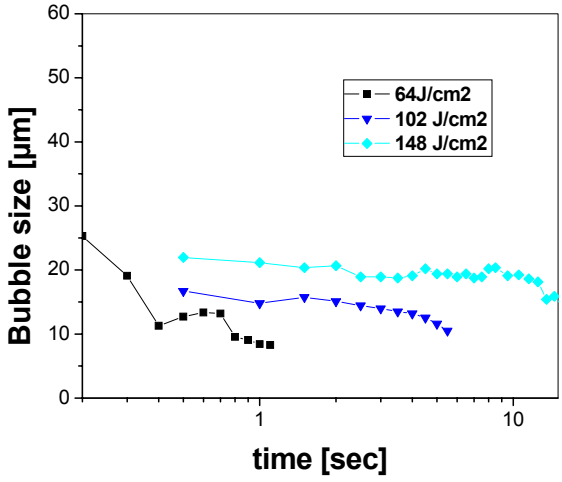

Figure 14. Bubble dynamics when bursts of femtosecond laser pulses are applied to transparent agar gels positioning the beam's waist 100 below the gel surface.

4 CONCLUSIONS

The type of bubble (transient or permanent) that can be produced by single 5 ns laser pulses is strongly dependent on the fluence of the pulse as shown in a previous work; however, for fluences under the threshold for permanent bubble formation, the type of bubble that can be formed depends on the number of pulses and the frequency at which these are

delivered. The fluence needed to form a bubble in highly scattering agar gel is ~50% more as that needed in clear agar gel at 50 and 100 μm deep. However, at 200 μm, at least 3 times higher fluence is required. Bubbles produced with femtosecond laser pulses with the fluences available in the laboratory were always transient and half the initial size than those produced with nanosecond laser pulses.

AKNOWLEGMENTS

1. *UCMEXUS-CONACyT Collaborative Research Grant,* "Studies of ultrashort laser pulse interaction with vascular and pigmented dermatologic lesions" with Dr. Santiago Camacho, CICESE, 07/01/04-08/30/06.

2. *UCR-Mexico Initiatives*, "Effects of ultrashort laser pulse irradiation on melanocyte viability", *UCMEXUS,* 09/01/04-04/30/06.

3. *NSF-SGER,* "Thermo-mechanical interactions of ultrashort laser pulses with subsurface targets of tissue models", *NSF* 07/01/06-06/30/07. Agency Award No: CTS-0609662.

4. CONACyT and UCMEXUS scholarship for graduate studies.

5. Mr. Gerardo Romo-Cardenas and Mrs. Alejandra Mina-Rosales for their collaboration in this work.

REFERENCES

1. Loo W.J., et al; "Recent advances in Laser therapy for the Treatment of Cutaneous Vascular Disorders", Lasers Med Sci, **17**, 9-12 2002,.
2. Venugopalan Vasan, et al. "Role of Laser-Induced Plasma formation in Pulses Cellular Microsurgery and Micromanipulation", Physical Review Letters, 88, 7, 88-7, 2002.
3. D. Du, et al**; "**Laser-Induced Breakdown by Impact ionization in SiO_2 With Pulse Widths from 7 ns to 150 fs**";** Appl. Phys. Lett., **64**, 3071-3073, 1994.
4. Anderson R.R and Parish J.S., "Selective Photothermolysis, precise microsurgery by selective absorption of pulsed radiation", Sience, **220**, 524-527, 1983.
5. Schuele Georg, et al.; "RPE Damage threshold and Mechanisms for Laser Exposure in Microsecond-to-Millisecond Time Regimen", Investigative Ophthalmology & Visual Science; **46**, 714-719, 1995.
6. Neumann Jörg, et al; "Boiling Nucleation on Melanosomes and Microbeads Transiently Heated by Nanosecond and Microsecond Laser Pulses", Journal of Biomedical Optics, **10(2)**, 024001-1-024001-12, 2005.
7. Ohl Claus-Dieter, et al; "Bubble Dynamics, Shock Waves and Sonoluminescence", Phil. Trans. R. Soc. Lond. A **357**, 269-294, 1999.
8. Laptko D. "Laser-Induced Bubbles in Living Cells". Lasers in Surgery and Medicine, **38**, 240-248, 2006.
9. Romo-Cárdenas Gerardo. et al, "Estudio de efectos foto-inducidos en modelos de tejido-biológico usando láser de nanosegundos"*; XVIII Congreso Nacional de Físca / XVIII Reunión Anual de Óptica;* Sociedad Mexicana de Fisica; Guadalajara, México; 2005.